Research Article | Vol. 12, No. 1 / 1 January 2021 / Biomedical Optics Express 272
Biomedical Optics EXPRESS

Detection of singlet oxygen luminescence for experimental corneal rose bengal photodynamic antimicrobial therapy

JEFFREY C. PETERSON,[1,2,3,7] ESDRAS ARRIETA,[1] MARCO RUGGERI,[1,2] JUAN D. SILGADO,[1] KEENAN J. MINTZ,[4] ERNESTO H. WEISSON,[3] ROGER M. LEBLANC,[4] IRENE KOCHEVAR,[5] FABRICE MANNS,[1,2,3] AND JEAN-MARIE PAREL[1,2,6,8]

[1]*Ophthalmic Biophysics Center, Department of Ophthalmology, Bascom Palmer Eye Institute, University of Miami Miller School of Medicine, 1638 NW 10th Ave, Miami, FL 33136, USA*
[2]*Department of Biomedical Engineering, University of Miami, 1251 Memorial Dr, Coral Gables, FL 33146, USA*
[3]*Miller School of Medicine, University of Miami, 1600 NW 10th Ave #1140, Miami, FL 33136, USA*
[4]*Department of Chemistry, University of Miami, 1301 Memorial Dr, Coral Gables, FL 33146, USA*
[5]*Wellman Center for Photomedicine, Massachusetts General Hospital, Harvard Medical School, 50 Blossom Street, Boston, MA 02114, USA*
[6]*Anne Bates Leach Eye Center, Department of Ophthalmology, Bascom Palmer Eye Institute, University of Miami Miller School of Medicine, 900 NW 17th St, Miami, FL 33136, USA*
[7]*petersonjeffreyc@gmail.com*
[8]*jmparel@med.miami.edu*

Abstract: Rose bengal photodynamic antimicrobial therapy (RB-PDAT) treats corneal infection by activating rose bengal (RB) with green light to produce singlet oxygen ($^1O_2$). Singlet oxygen dosimetry can help optimize treatment parameters. We present a $^1O_2$ dosimeter for detection of $^1O_2$ generated during experimental RB-PDAT. The system uses a 520 nm laser and an InGaAs photoreceiver with bandpass filters to detect $^1O_2$ luminescence during irradiation. The system was validated in RB solutions and *ex vivo* in human donor eyes. The results demonstrate the feasibility of $^1O_2$ dosimetry in an experimental model of RB-PDAT in the cornea.

1. Introduction

Corneal infection (keratitis) is a common ocular emergency which can lead to permanent damage to the cornea and possible blindness and complete loss of the eye due to endophthalmitis [1]. There are various antimicrobial drugs to fight these infections, but they often have limited success treating resistant or atypical organisms [2,3].

Preliminary studies demonstrate the potential of Rose Bengal Photodynamic Antimicrobial Therapy (RB-PDAT) as a therapy for treating microbial keratitis [4–8]. The infected portion of the cornea is treated with the photosensitive dye Rose Bengal (RB), then exposed to 500–560 nm light. Reactive singlet oxygen ($^1O_2$) generated by this process destroys the infecting microorganisms [9,10]. While preliminary results have been promising (>80% of patients treated with experimental RB-PDAT avoid emergency cornea transplant), a better understanding of the fundamental photochemical processes for generating $^1O_2$ is required to maximize treatment efficacy [8]. The goals of the optimization include maximizing $^1O_2$ production, maximizing treatment depth, and minimizing treatment time [11,12]. To make this possible, an accurate measure of $^1O_2$ dose must be established.

$^1O_2$ dose can be quantified by measuring 1270 nm luminescence [13,14]. However, this method is technically challenging within biological environments due to extremely weak emission

#405601 https://doi.org/10.1364/BOE.405601
Journal © 2021 Received 26 Aug 2020; revised 19 Oct 2020; accepted 25 Oct 2020; published 10 Dec 2020

Biomedical Optics EXPRESS

[15–21]. As a result, highly sensitive detection systems, sometimes combined with time-gating, are required [13,22–30]. Due to their complexity it would be challenging to integrate these detectors into a clinical system adapted toward $^1O_2$ measurements in the human cornea.

Recently, dosimetry systems have been developed using InGaAs cameras and photoreceivers, which are able to measure real-time continuous wave emission at sensitivity levels approaching that of photomultiplier tubes [13,22–24,31–35]. While InGaAs avalanche diodes might still use time-gating, most of these systems perform continuous wave measurements, relying purely on spectral filtering to select for $^1O_2$ luminescence at approximately 1270 nm. Several of these devices have successfully measured $^1O_2$ production in the skin *in vivo* [22,36]. To date however, no system has been specifically built for the purposes of $^1O_2$ measurement in the corneal surface during experimental RB-PDAT.

In this work we present a proof-of-concept system for corneal $^1O_2$ measurement. This study relies on methods demonstrated in previous work for animal models, which use continuous-wave photosensitizer excitation and $^1O_2$ measurement using spectral filtering with an InGaAs photodetector [36]. While these works focus primarily on measurements of skin or superficial tumors, our $^1O_2$ dosimeter is focused specifically on $^1O_2$ luminescence measurement during experimental corneal RB-PDAT. The system generates $^1O_2$ using a continuous-wave 520 nm laser excitation source to stimulate RB solutions and human donor eyes treated with RB photosensitizer. Optical filters provide spectral separation between collected $^1O_2$ luminescence (approximately 1270 nm) and background fluorescence from RB and/or tissue autofluorescence. The goal of this study was to demonstrate feasibility of this approach for corneal surface $^1O_2$ luminescence dosimetry.

2. Description of a singlet oxygen $^1O_2$ dosimeter

A 520 nm, 4.5 mW diode laser emitting a 4.6 mm x 1.7 mm elliptical beam (CPS520, Thorlabs) was used. Laser emission is controlled manually using a shutter (Fig. 1). Preliminary testing of the laser showed some residual IR emission. Therefore, the laser light is filtered to remove residual IR emission using a glass filter (FGS900-A, Thorlabs). The laser light passes through a dichroic shortpass filter (#86-697, Edmund Optics). This dichroic filter transmits the incident green laser beam and reflects light with wavelengths above 1155 nm toward the detector, which includes $^1O_2$ luminescence (approximately 1270 nm). The laser is focused with a 20x objective lens (W.D. = 3.2 mm, N.A. = 0.4, f = 9.0 mm), onto the sample (Fig. 1, Lens 1). The calculated spot size of the beam is 3.5 µm × 1.3 µm, assuming that the focused beam is Gaussian and diffraction limited. The corresponding peak irradiance, not accounting for transmission losses, is 2.5×10^5 W/cm^2. The near infrared radiation emitted by the sample is collected by the same lens and reflected by the dichroic filter through a sliding filter holder. In order to spectrally separate $^1O_2$ luminescence (approximately 1270 nm) from RB fluorescence and/or tissue autofluorescence and observe a $^1O_2$ luminescence peak, four bandpass filters were accommodated in the sliding filter holder (1200, 1250, 1277, and 1300 nm, with FWHM of 10, 10, 20, and 12 nm, respectively. All filters were purchased from Edmund Optics, except the 1277 nm filter, which was purchased from Omega Optical). The 1277 nm bandpass filter selects for $^1O_2$ luminescence, while the other bandpass filters (1200, 1250, and 1300 nm) provide a measurement for RB fluorescence and/or tissue autofluorescence within this range. The 1277 nm filter was chosen as the closest off-the-shelf available filter for $^1O_2$ luminescence measurement. Since the $^1O_2$ luminescence is a weak signal that may be masked by these intrinsic fluorescence sources, two 1150 nm longpass filters are stacked in the detection path. The light transmitted by the filters is then focused with a plano-convex lens (Lens 2, f = 8 mm, ACL12708U-C-SP, Thorlabs) onto an InGaAs photoreceiver with femotwatt sensitivity (PDF10C, Thorlabs).

Biomedical Optics EXPRESS

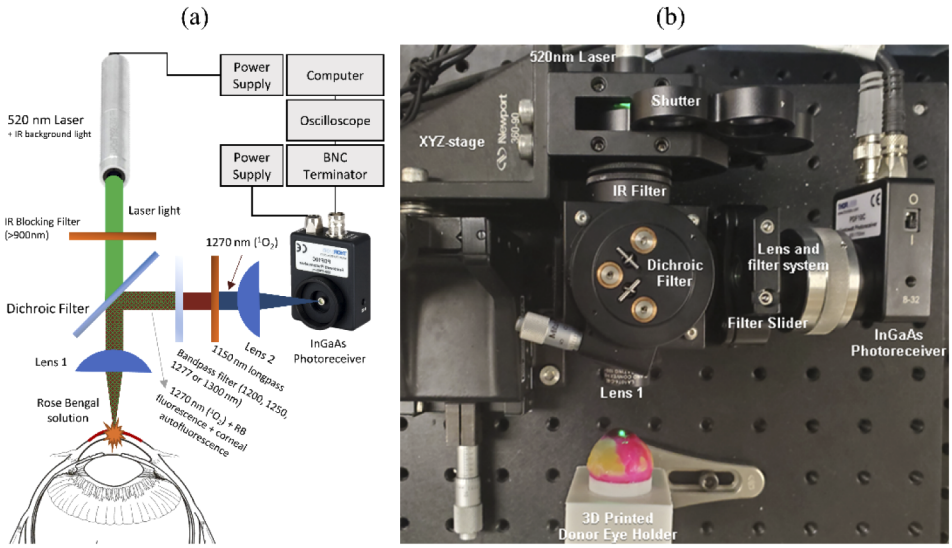

Fig. 1. (a) Schematic of proof-of-concept corneal $^1O_2$ dosimetry system (b) Experimental setup for measurement of *ex vivo* human donor eyes.

To ensure proper alignment of the optics and maximize signal detection, the dichroic filter is placed on a stage capable of fine rotation up to ± 7°, and both the collecting lens and focusing lens have been mounted such that their axial positions are adjustable by ± 1.5 mm.

The InGaAs photoreceiver was connected through a 75 Ω BNC cable to a resistance terminator (10 kΩ) to prevent RF signal reflection and reduce noise, and then to an oscilloscope (PicoScope 2204A, Pico Technology). Finally, the oscilloscope signal is recorded with a computer and processed in MATLAB 2019a (MathWorks, Natick, MA, USA).

3. Data collection and processing

In all experiments, the $^1O_2$ luminescence is measured using the same procedure. At least 15 minutes before any measurement, with the shutter closed, the 520 nm laser and the InGaAs photoreceiver are turned on to allow time for warm-up as recommended by the manufacturers. The 1277 nm bandpass filter is placed in the detection arm. The sample is mounted onto the optical bench in front of Lens 1. The room lights are then turned off and the laser shutter is opened. The dosimeter is precisely positioned in front of the sample using the XYZ linear translation stage until the signal detected is maximized. The background signal recorded for two seconds. The shutter is then opened, and the recording continues for approximately 15 seconds (Fig. 2). The 1277 nm bandpass filter is then removed and replaced with one of the other filters. This procedure is repeated three times for each bandpass filter. The oscilloscope records data at 750 Hz.

The recorded signal is filtered using a 50 Hz low-pass filter to remove 60 Hz AC noise. Immediately after the laser shutter is opened, some of the measured signals include an initial decay phase (Fig. 2). This initial decay phase is most obvious in measurements at 1277 nm and is thought to be due to $^1O_2$ luminescence decrease due to decreased oxygen supply within the tissue [37]. To have a more reliable comparison between measurements, only the data after the decay phase, from 3.5 to 16.5 s, were used in the analysis. The averaged background signal from each recording is subtracted from the average signal measurement. These data are then corrected for the transmission provided by the manufacturer for each bandpass filter.

Biomedical Optics EXPRESS

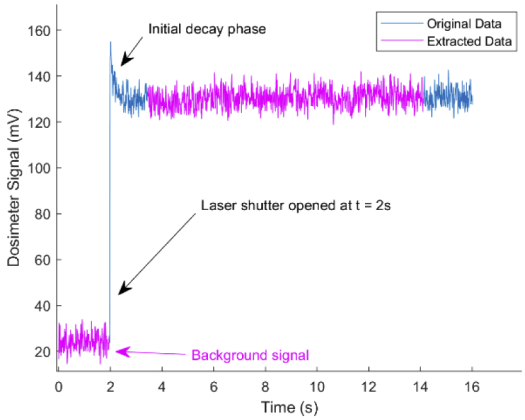

Fig. 2. Example raw signal collected from the experiment outlined in Section 4.1 (1277 nm bandpass signal for 0.1% Rose Bengal in distilled water measured in cuvette).

4. Validation of the dosimeter

4.1. Measurements of $^1O_2$ luminescence in solution

In order to verify if the dosimeter can measure $^1O_2$ luminescence, we first tested the device on solutions of Rose Bengal contained in a 1 cm optical cuvette mounted in a custom designed holder. The cuvette is held approximately at a 25° angle to prevent back reflection of the laser generated by the window surface into the objective lens (see Fig. 3(a)). XYZ position of the dosimeter in front of the cuvette was set by finding where the signal was maximum using the 1277 nm BP filter with a solution of 0.1% RB in distilled water (18 MΩ-cm resistivity, NERL High Purity Water, Thermo Scientific). We performed five experiments measuring $^1O_2$ luminescence using triplicate measurements.

1. 0.1% RB in distilled water: to determine if a $^1O_2$ luminescence peak near 1277 nm could be observed in RB solution that is given to patients for RB-PDAT.
2. 0.1% RB in $^1O_2$ "booster" (heavy water, 99% D_2O): to increase $^1O_2$ signal to confirm the peak near 1277 nm is $^1O_2$ luminescence and not due to RB fluorescence and/or back reflected laser light [15,38].
3. 0.1% RB in $^1O_2$ quencher (200 mM sodium azide, NaN_3): to decrease $^1O_2$ signal to further confirm the peak near 1277 nm is caused by $^1O_2$ luminescence [37,39].
4. 99% D_2O: to provide a measurement of how much of the signal was due to back reflection of the 520 nm laser and confirm no 1277 nm peak is observed when RB is not present in solution.
5. Distilled water: to provide a measurement of back reflection of the 520 nm laser and confirm no 1277 nm peak is observed when RB is not present in solution.

In Fig. 3(b), the peak at 1277 nm closely matches the reference $^1O_2$ spectrum for the 0.1% RB in D_2O solution [40]. Combined with the increased peak using D_2O and the decreased peak from NaN_3, these results show that the dosimeter is measuring $^1O_2$. The signal that remains for the 0.1% RB in 200 mM NaN_3 solution after quenching is assumed to be background signal due to RB fluorescence [36]. Subtracting this RB fluorescence background signal from the 1277 nm signal for the 0.1% RB in distilled water and 0.1% RB in D_2O solutions, we estimate that 79% and 92% of the 1277 nm signal can be attributed to $^1O_2$ luminescence, respectively.

Biomedical Optics EXPRESS

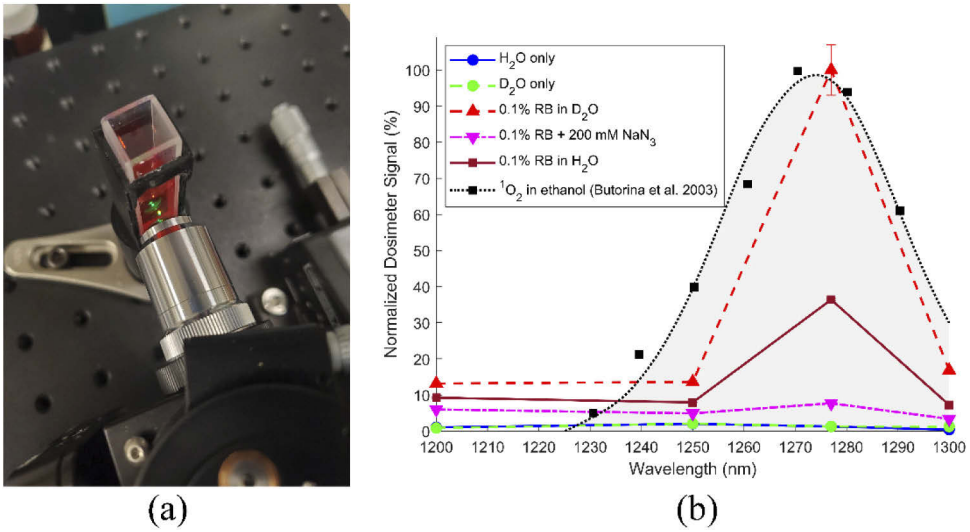

Fig. 3. (a) Experimental setup for solution measurement. (b) Results of the dosimeter *in vitro* experiment comparing cuvette measurements for solutions of distilled water only, D_2O only, 0.1% RB in distilled water, 0.1% RB in D_2O, and 0.1% RB in 200 mM NaN_3. Note that 0.1% RB corresponds to 1.03 mM RB. Three measurements were taken using bandpass filters at 1200, 1250, 1277, and 1300 nm. Normalized average dosimeter voltage signal is displayed, where 100% corresponds to 293.4 mV or 3.99×10^{12} $^1O_2$ molecules per second (calculated, see appendix). In addition, a sample $^1O_2$ spectrum is displayed for comparison [40]. Note that all data points have error bars, however almost all are too small to be visible beyond the data point marker.

4.2. *Effect of RB concentration on $^1O_2$ signal*

We sought to determine if the system could successfully record $^1O_2$ luminescence signals for a range of RB concentrations that are relevant to clinical use. In order to test this, we performed an *in vitro* experiment comparing dosimeter signals with varying RB concentrations in distilled water in a glass cuvette as described in the previous section: 0%, 0.05%, 0.10%, 0.15%, and 0.20%. These concentrations were chosen because this is the RB concentration range that has been shown to have clinically relevant antimicrobial effect [4,5,8,41,42]. Prior studies have demonstrated that lower concentrations do not produce an efficient antimicrobial effect. The setup and measurement were the same as shown in Fig. 3(a).

Normalized $^1O_2$ dosimeter signal is shown in Fig. 4. Signal at 1277 nm decreased with increasing RB concentration. All RB solutions had highest signal at 1277 nm compared to other measured wavelengths. $^1O_2$ dosimeter signal likely decreased with increasing RB concentration, which is explained by the formation of aggregates at high concentration of RB inducing self-quenching [43–46]. It is likely that the signal at 1277 nm would have increased at concentrations of RB lower than 0.05%, and that 1277 nm signal would show a positive trend at RB concentrations below 0.015% (150 µM), above which self-quenching RB multimers are thought to begin forming in solution [43]. Attenuation of the 1277 nm light directly due to increasing RB concentration is unlikely to be a contributing factor because RB is nearly transparent to 1277 nm light even at concentrations as high as 10 wt% RB [47].

Biomedical Optics EXPRESS

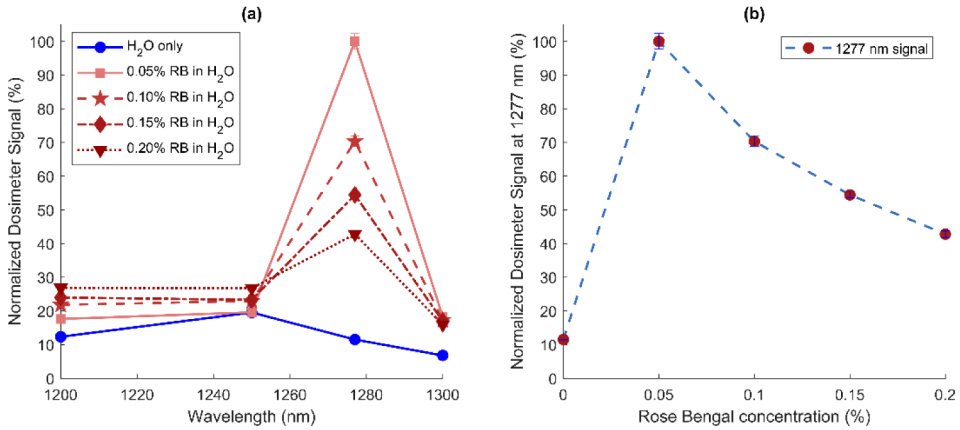

Fig. 4. (a) Results of the dosimeter *in vitro* cuvette experiment comparing dosimeter signal of solutions of 0%, 0.05%, 0.10%, 0.15%, 0.20% RB in H_2O. (a) Three measurements were taken with each bandpass filter at 1200, 1250, 1277, and 1300 nm for each solution. Normalized average dosimeter voltage signal is displayed, where 100% corresponds to 165.2 mV or 2.25×10^{12} $^1O_2$ molecules per second (calculated, see appendix). Note that all data points have error bars, however almost all are too small to be visible beyond the data point marker. (b) Signal measured using 1277 nm BP filter.

4.3. Measurements of $^1O_2$ luminescence in human donor eyes

4.3.1. Purpose and methods

To determine if the $^1O_2$ dosimeter can detect $^1O_2$ luminescence during RB-PDAT in the cornea, we tested the $^1O_2$ dosimeter using five human donor eye pairs (ten eyes) treated with solutions of RB. See Table 1 for a summary of different treatment conditions.

Table 1. Treatment Conditions for Whole Globe Experiment

Group label	# eyes measured	Post-mortem time (days)	Dextran Treatment	Rose Bengal application	0.1% Rose Bengal solvent
Group 1	3	4,17,18	--	Sponge presoaked with RB; RB then applied with 10 G pipette every 3 min for 30 min	--
Group 2	7	4,4, 10,10,17,18,18	20% dextran in distilled water/D_2O/200 mM NaN_3		--
Group 3	3	4, 9, 18	20% dextran in D_2O		D_2O
Group 4	3		20% dextran in 200 mM NaN_3		200 mM NaN_3
Group 5	3	10, 10, 17	20% dextran in distilled water		Distilled water

All measurements were performed in triplicate at the same XYZ location on the cornea. The system collects luminescence from the corneal surface through a corneal depth of approximately 150–200 µm. The XYZ location was stimulated for approximately 3 to 4 minutes in total in order minimize the effects of photobleaching. Due to the manual operation of the system, each triplicate measurement required approximately 30 minutes including positioning and alignment of the eye and irradiation. Despite possible non-uniformity of corneal RB distribution, multiple XYZ locations were not used due to concerns that excessive measurement time would become a confounding variable.

1. Group 1 – no treatment (3 eyes): serves as a baseline measurement of how much of the signal corresponds to back reflection of the 520 nm laser and/or tissue autofluorescence.

Biomedical Optics EXPRESS

2. Group 2 – 20% dextran treatment (7 eyes): serves as a baseline measurement of how much of the signal corresponds to back reflection of the 520 nm laser and/or tissue autofluorescence, as well as how much dextran affects measured signal.

3. Group 3 – 0.1% RB in $^1O_2$ "booster" (heavy water, 99% D_2O) (3 eyes): due to high quenching by tissue, D_2O was used to boost $^1O_2$ signal sufficiently to obtain a measurement on cornea [15,19,37]. The second purpose was to verify we are measuring $^1O_2$ luminescence by observing a signal boost at 1277 nm compared to the clinical solution (0.1% RB in distilled water). 0.1% RB is the concentration of RB that is most commonly used in clinical application [4,5,8,41,42].

4. Group 4 – 0.1% RB in $^1O_2$ quencher (200 mM sodium azide, NaN_3) (3 eyes): to decrease $^1O_2$ signal to further confirm the peak near 1277 nm is $^1O_2$ [39].

5. Group 5 – 0.1% RB in distilled water (3 eyes): Determining if $^1O_2$ luminescence could be observed in RB solution that is given to patients for RB-PDAT.

6. 16-minute duration measurement of group 3 (0.1% RB in D_2O) at 1277 nm: the purpose was to observe how much of an effect photobleaching had on measurements by observing signal decrease at 1277 nm over a 16-minute period. Group 3 was used because the D_2O solvent would maximize the chance that $^1O_2$ would cause photobleaching (D_2O increases $^1O_2$ lifetime) [15]. Oscilloscope data acquisition was adjusted to 300 Hz for this measurement. To confirm that the decrease in power was not caused by the laser instability, we performed a separate measurement of the laser power stability for 45 minutes and measured 0.27% power variation during that window. This confirms that that laser instability did not play a role in signal decrease during this experiment.

Corneal preparation: Donor eyes not suitable for clinical use were graciously provided by the Florida Lions Eye Bank located at Bascom Palmer Eye Institute. Eyes were used between 4 and 18 days after donor death, with a median eye post-mortem time of 10 days. Eyes were cleaned of extraocular tissue and then placed in a custom 3D printed vacuum holder to allow for easy handling (Fig. 5). The epithelium in all corneas was debrided (de-epithelialized) to a diameter of 8 mm. To restore a normal intraocular pressure (IOP), 0.9% NaCl (1-1.5 mL) was injected into the vitreous humor through the optic nerve using a 27 G needle. To both clarify the cornea and bring it to a physiologic thickness, a small volume (approximately 50 µL, or until cornea was taut) of 20% dextran solution was injected into the anterior chamber using a 25 G needle. Like the corresponding RB solution, the 20% dextran solution was prepared using approximately 40 kDa dextran (D1662, Sigma-Aldrich) in a solvent of either D_2O, 200 mM NaN_3, or distilled water. The eye was then placed face down in a pool of 20% dextran solution for 60 minutes. A custom eye holder with a cylindrical well filled with 20% dextran solution was created to ensure only the cornea was exposed to dextran. To verify that the corneal thickness and pressure reached physiologic values, triplicate pachymetry (Accutome PachPen Pachymeter 24-510) and tonometry (Clement-Clarke Perkins MK2 Handheld Tonometer) measurements of the donor eyes were performed, respectively, after removal of epithelium and after 60 minutes of 20% dextran treatment. After all preparation steps, corneal thickness was measured as less than 599 µm for all but 3 eyes (one eye each in groups 3–5), and IOP ranged from 0–74 mmHg for all eyes. Low IOP in two eyes (one each in groups 3 and 5) resulted from leakage from the tissue surface after the initial saline injection. However, IOP should not have significant effect on luminescence measurements because it is the $^1O_2$ generated by RB, not the corneal tissue, which produces the luminescence. To apply RB solution, a 6 mm corneal sponge was presoaked with RB, then placed on the corneal surface. RB was applied for 30 minutes, with three drops added every 3 minutes using a 10 G pipette. After RB treatment, the corneas were washed with 0.9% NaCl.

Biomedical Optics EXPRESS

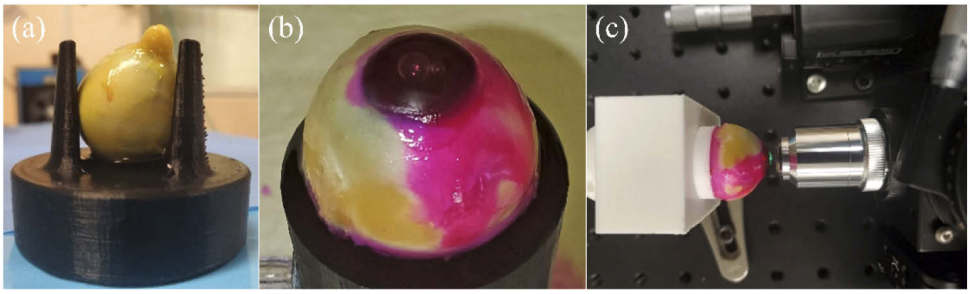

Fig. 5. Steps for preparation and treatment of whole eyes (a) Eye from group 3 placed face down in 3D printed holder for 60 minutes in well of 20% dextran solution. (b) Eye from group 3 with corneal RB staining after RB treatment. (c) Eye from group 3 placed into 3D printed vacuum holder for $^1O_2$ luminescence measurement. Approximately 80% of RB remains in the most superficial 70 µm of the cornea, and maximum RB depth ranges from approximately 70–150 µm [39,50–52].

$^1O_2$ measurement: Similar to the *in vitro* experiments, whole globes were first placed in a custom holder and mounted in the system. Alignment was accomplished by adjusting XYZ position to the point of maximum signal in the RB stained region of the eye using the 1277 nm bandpass filter. All eyes were measured three times with each bandpass filter (1200, 1250, 1277, and 1300 nm). All eyes from group 1 were measured before any treatment. In group 2, all eyes were measured after 20% dextran treatment. Groups 3, 4, and 5 were measured after RB treatment.

Photobleaching measurement: After $^1O_2$ measurements using all four bandpass filters, $^1O_2$ dosimeter signal was measured at a new RB stained section of the cornea. The signal was measured at 1277 nm over a 16-minute period for group 3 (treated with 0.1% RB in D_2O) sampled at 300 Hz. Hydration of the cornea was not maintained during this period, which may have resulted in decreased signal due to changes in tissue properties and corneal thickness [48,49]. Because there is an initial spike in the measured signal (see Fig. 2), the first recorded 10 seconds of data was removed to more clearly observe photobleaching.

4.3.2. Results and discussion

$^1O_2$ dosimeter results are shown in Fig. 6. All RB treated groups had an increased 1200 nm signal compared to signal at 1250 nm. Measuring group 3 over a 16-minute period showed a linear decrease in 1277 nm signal for all eyes (Fig. 7).

The spectral measurements from the whole donor eyes showed significantly increased signal at 1277 nm for the 0.1% RB treated groups 3, 4, and 5 compared to groups 1 and 2. Between the RB treated groups, 0.1% RB in D_2O had the highest mean signal at 1277 nm, followed by 0.1% RB in H_2O and finally 0.1% RB in NaN_3. However, these differences were not statistically significant. Quenching by NaN_3 did not decrease luminescence and use of D_2O did not increase luminescence, possibly due to higher RB concentration in the cornea or rapid quenching of $^1O_2$ by corneal collagen (see next section) [39]. RB is strongly associated with collagen in cornea, thus the $^1O_2$ is generated very close to the protein and may react with nearby amino acids of the collagen chains. This would shorten the $^1O_2$ lifetime, making it less likely to encounter, and be quenched by, azide. Consequently, in cornea, sodium azide may not be an efficient quencher of $^1O_2$. Similarly, while D_2O increases $^1O_2$ signal in solution compared to H_2O by lengthening $^1O_2$ lifetime (due to less efficient vibrational coupling of $^1O_2$ with D_2O), rapid reaction of $^1O_2$ with nearby amino acid dramatically reduces $^1O_2$ lifetime, thus negating the signal boosting effects of D_2O observed in solution. As in the *in vitro* studies, the dosimeter signal from 1250 to 1300 nm

Biomedical Optics EXPRESS

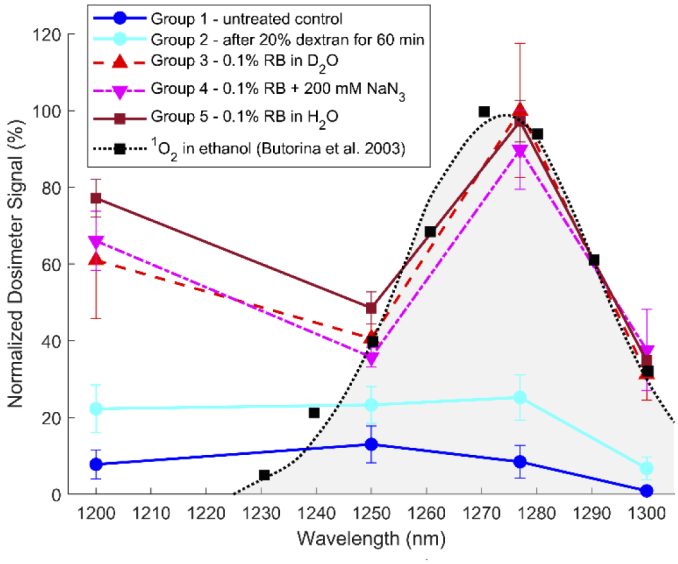

Fig. 6. Whole eye dosimeter measurements compared to $^1O_2$ reference spectrum [40]. All data points have error bars but are not visible due to small 95% standard deviation. Normalized average dosimeter voltage signal is displayed, where 100% corresponds to 144.0 mV or 1.96×10^{12} $^1O_2$ molecules per second (calculated, see appendix).

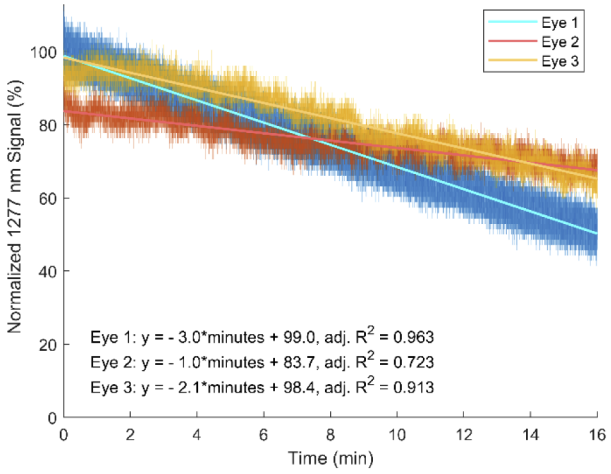

Fig. 7. Dosimeter signal at 1277 nm for group 3 (treated with 0.1% RB in D_2O) measured over 16 min at 300 Hz. A linear decrease is observed for all eyes.

appears to closely match the $^1O_2$ spectrum from Butorina et al. with the exception of the signal at 1200 nm [40]. Despite the failure to significantly quench or boost $^1O_2$ signal in corneas, the clear peak at 1277 nm demonstrates that we are successfully measuring $^1O_2$ [26].

Although repeat studies and RB fluorescence measurements to determine local RB concentration are necessary, our preliminary results suggest photobleaching appears to progressively reduce the luminescence intensity over the course of 16 minutes. As RB is photobleached, it can no longer generate $^1O_2$ and no RB can diffuse to replace the photobleached molecule because the majority of the RB is fixed in place bound to stromal collagen [53]. As a result, the $^1O_2$ luminescence

Biomedical Optics EXPRESS

signal depletes over time as more RB molecules are continually deactivated. Another possible explanation for these results is that the cornea continued to thin during measurement, causing the corneal surface to gradually move away from the dosimeter focal plane. Extrapolating these data, we can infer that the measurements shown in Fig. 6 were subject to less than 15% drop in signal strength over the 3 to 4 minute measurement window, which is not significant enough to alter the conclusions of this study.

5. Discussion

To the best of our knowledge, this is the first direct measurement of singlet oxygen ($^1O_2$) luminescence in corneal tissues. While this work uses a detection scheme presented in other works, this is the first application to corneal $^1O_2$ measurement using Rose Bengal photosensitizer [28–30,36]. We present a $^1O_2$ dosimeter system that uses an in-line excitation laser and a fixed-gain, room-temperature InGaAs photoreceiver to measure $^1O_2$ generated from RB in solution and during experimental RB-PDAT in human donor eyes. Our results indicated a clear luminescence peak near 1277 nm that increases in the presence of a $^1O_2$ booster (D_2O) and decreases in the presence of $^1O_2$ quencher (NaN_3) in solution. In addition, we were able to characterize $^1O_2$ signal from a range of clinically relevant concentrations of Rose Bengal.

In order to use this dosimetry system to measure the dose of $^1O_2$, we must convert the measured luminescence to a quantity of $^1O_2$. As discussed in Appendix 1, for this setup it is calculated that $1\,V \approx 1.36 \times 10^{10}$ $^1O_2$ molecules generated in the measured sample volume. This calculation is useful because, in addition to providing us with a measurement of $^1O_2$ content, it also allows us to perform direct comparisons with results from theoretical models for photodynamic therapy, as well as comparison with other dosimeters [25,54,55].

Comparing the *ex vivo* whole eye measurements to *in vitro* measurements, we see an increased 1200 nm signal *ex vivo*. We suspect this is due to the effects of performing these measurements in tissue. It is known that RB binds tightly with collagen, and the resultant local concentration of RB in the corneal stroma is much higher than in solution [39,53]. At the same time, there is potentially shorter $^1O_2$ lifetime in collagen matrix compared to in distilled water, so $^1O_2$ signal within the cornea is lower for a given RB concentration [15–21]. Thus, we would expect a large increase in RB fluorescence to be observed even at 1200 nm, with only a moderate change in $^1O_2$ signal at 1277 nm. On the other hand, signal increase for all wavelengths for the 20% dextran treated control eye is likely due to decreased scattering, and therefore increased back reflection of 520 nm laser light [48,56–59].

However, compared to the *in vitro* study, there was not a significantly increased signal for the 0.1% RB in D_2O treated samples compared to 0.1% RB in distilled water. In addition, there was no decrease in 1277 nm signal for the eye treated with NaN_3. Collagen is known to react with and quench $^1O_2$, so that also is likely contributing to reduced $^1O_2$ signal [16]. Because RB is strongly associated with collagen in the cornea, $^1O_2$ is produced in proximity to nearby amino acids of the collagen chains. $^1O_2$ reacts with these nearby amino acids, making it less likely to interact with NaN_3 or D_2O. In addition, the local concentration of RB at the corneal surface is much higher than the concentration in solution due to the favorable interaction between RB and collagen [39]. This higher RB concentration would result in higher $^1O_2$ production despite the lower measured luminescence signal. This higher $^1O_2$ production might be outpacing the rate of quenching by NaN_3, and thus no significant difference is observed. In addition, a higher RB concentration at the corneal surface may be lowering $^1O_2$ luminescence in all studies, both due to attenuation of light, preventing excitation of RB deeper in the cornea, as well as due to self-aggregation behavior of the RB dye [39,43,46].

The human donor eyes in this study were measured between 4–18 days after donor death. This long post-mortem interval likely allowed some collagen breakdown within the cornea while stored at 4°C [60,61]. If so, the collected $^1O_2$ luminescence signal might be lowered due to the

Biomedical Optics EXPRESS

exposure of more His and Tyr residues which readily react with $^1O_2$, thus reducing the its lifetime [16,62–65]. Furthermore, $^1O_2$ reaction with ascorbate within the cornea may affect the collected $^1O_2$ luminescence [66,67]. The concentration of ascorbate would be expected to decrease due to oxidation during the post-mortem period, thus increasing collected $^1O_2$ luminescence. Taken together, we might expect to see small changes in $^1O_2$ luminescence from a long post-mortem interval. Finally, higher quality corneas are usually reserved for transplantation. It is possible the quality of the received tissue or the cause of death could have impacted the results. However, none of these effects should change the overall trends observed in the measured results.

The attenuation coefficient of a healthy cornea around 500-550 nm (<10 cm^{-1}) is potentially orders of magnitude lower than the attenuation coefficient of 0.1% RB treated corneal tissue (46–2,300 cm^{-1}, depending on the estimated RB concentration in cornea) [39,53,68,69]. Additionally, in healthy cornea the attenuation coefficient around 1000 nm is <1.4 cm^{-1} [70]. We therefore do not expect that attenuation of green light or $^1O_2$ luminescence by the cornea will have a significant effect on the outcome. Additional attenuation may be present in vivo in a diseased cornea due to increased scattering. Assuming scleral tissue would have similar optical properties to diseased cornea (approximate attenuation at 500 nm is <10 cm^{-1} and at 1050 nm is <2 cm^{-1}), we still expect that the attenuation will be dominated by Rose Bengal given its very high absorption [71,72].

Though the system demonstrated successful $^1O_2$ luminescence measurement, a more rigorous study with larger sample size will be required to establish more robust values for $^1O_2$ concentrations generated in the cornea. In addition, to reduce differences in measurements due to sample variation, future studies should measure the same eyes before and after treatment in a matched-pair study design. While at least three eyes were measured per treatment group, small sample size was a significant limitation of the study, which is not able to account for variance between donor eyes, in experimental and surgical technique, and heterogeneity of RB distribution on the corneal surface. While some variation has been observed in studies on *ex vivo* and *in vivo* rabbit corneas, differences between samples would not be expected to significantly impact outcomes for this proof-of-principle study [39,50,51].

To ensure that there is sufficient concentration of $^1O_2$ booster and quencher in the cornea, a higher NaN_3 concentration and a 24 hour corneal soaking period in 20% dextran solution will need to be used in future studies [48,56]. Lastly, it is clear that photobleaching plays a role in these measurements. This aspect of the study needs to be controlled for in future studies by measuring at different locations on the cornea, as well changing around the order of measurements so as not to favor the result from any one bandpass filter.

The current system shows the feasibility for experimental studies on cadaver eyes which will help optimize RB-PDAT treatment parameters. Ideally, this system would be used during clinical RB-PDAT application to monitor $^1O_2$ dose. To realize this goal, successful measurement of $^1O_2$ luminescence will need to be established using the clinical RB-PDAT light source (525 nm LED source, 6–16 mW/cm^2) [8]. This clinical light source has 10^7 times lower irradiance than the focused 520 nm, 4.5 mW laser presented in this study, but this is mitigated to some extent because a much larger volume of the cornea would be irradiated and measured. Experiments will need to be carried out to verify successful $^1O_2$ luminescence measurements using the clinical source at these lower irradiance levels. In addition, to bring the system closer to *in vivo* and clinical use, a longer focal length lens will need to replace the current 20× objective for Lens 1. This will minimize errors due to small movements of the subject. Finally, the system will need to be transferred to a free-standing configuration that can be integrated within the clinical RB-PDAT delivery system so that it can more easily perform measurements on subjects.

A general limitation of the current dosimeter design is that it is only capable of measuring one small spot, failing to capture the entire picture across the cornea. Rose Bengal distribution can vary along the corneal surface, and so a 2D image of corneal $^1O_2$ may prove valuable. A

Biomedical Optics EXPRESS

near-infrared camera or scanning based system instead of the current fixed-position InGaAs photoreceiver detection might be a better able to obtain a more complete picture of the distribution of $^1O_2$ across the corneal surface [22,73].

A final limitation of our dosimeter is that it is unable to provide information on RB-PDAT dose at different corneal depths, which becomes important for deep invading organisms such as *Fusarium* or *Acanthamoeba* [11,12].

6. Conclusion

We present the design of a dosimeter for use in experimental RB-PDAT. Our studies show that the system can be used to measure $^1O_2$ luminescence. The device will be used in further studies to optimize treatment parameters. In addition, a next step will be to demonstrate the feasibility of using $^1O_2$ luminescence measurements to estimate the efficiency of RB-PDAT.

Appendix 1

The number singlet oxygen molecules produced per second in the measured volume, $n_{^1O_2}(t)$, is proportional to measured luminescence signal $L_{measured}(t)$ (photons s^{-1} @ 1277 nm) as described by Eq. (1):

$$n_{^1O_2}(t) = \frac{\tau_L * L_{measured}(t)}{f_{collected}} \tag{1}$$

where $\tau_L = {k_L}^{-1}$ is the luminescence lifetime ($\tau_L = 5.55$s for $^1O_2$ in water) and $f_{collected}$ is the fraction of generated photons that are collected by the system [55]. While τ_L was determined in water, it does not change with differing media [27,55,74].

Calculation of $f_{collected}$ is based on product of the transmission and numerical aperture of the optical system at 1277 nm. Total transmission of the optics at 1277 nm is approximately 69%, and the numerical aperture of Lens 1 = 0.4. The fraction of the total luminescence output collected by Lens 1 is calculated by dividing the solid angle collected by Lens 1 (a function of NA) by the solid angle of the sphere of isotropic $^1O_2$ luminescence (4π). For our setup, $f_{collected}$ is approximately 2.9×10^{-2}. The conversion from signal to $^1O_2$ dose assumes that the value of the collection efficiency is constant across experiments. In the present study we used a microscope objective with high numerical aperture (NA = 0.4) to collect the signal. Due to the high numerical aperture, the system will be more sensitive to axial positioning errors, which may produce variations in the collection efficiency. In clinical use, a significantly lower numerical aperture providing a significantly longer depth of focus will be implemented to meet the requirement for a longer working distance. The clinical system will therefore be less sensitive to variations in position and provide a more reliable conversion factor. Finally, $L_{measured}(t)$ can be calculated based on the characteristics of the InGaAs photoreceivers:

$$L_{measured}(t) = \frac{V_{OUT}}{R(\lambda) * G * h\nu} \tag{2}$$

where $L_{measured}(t)$ is optical power incident on the photoreceiver (photons s^{-1}), V_{OUT} is the measured output voltage (V), $R(\lambda)$ is responsivity of the photoreceiver at a given wavelength (approximately 0.9 A/W @ 1277 nm), G is detector gain (10^{11} V/A ± 10%) and $h\nu$ is the photon energy at 1277 nm (1.56×10^{-19} J). With these parameters and combining Eq. (1) and (2), we find:

$$n_{^1O_2}(t) = 1.36 \times 10^{10} * V_{OUT} \tag{3}$$

Equation (3) allows us to calculate the instantaneous number of $^1O_2$ molecules present in the measured volume based on the dosimeter voltage signal, as well as properties of the InGaAs photoreceiver and system optics. The value in Eq. (3) could be converted to μM by dividing

Biomedical Optics EXPRESS

$n_{^1O_2}(t)$ by the relevant phantom volume (i.e. volume over which $^1O_2$ luminescence reaches the InGaAs detector).

To determine the cumulative $^1O_2$ dose, $^1O_{2,dose}$, Eq. (3) can be integrated over the length of the collection period, t:

$$^1O_{2,dose} \equiv \frac{1}{\tau_D} \int_0^t n_{^1O_2}(t)dt \tag{4}$$

τ_D is measured $^1O_2$ lifetime within a given media [27,37,55]. For tissue, $\tau_D \approx 30$–180 ns, for pure H_2O $\tau_D \approx 4$ µs, pure D_2O $\tau_D \approx 68.1$ µs and for 200 mM NaN_3 in H_2O, τ_D is calculated ≈ 185 ns [19,37,75].

Funding

NIH Center Grant (P30EY14801); Donations from Drs. H.W. Flynn Jr, K. R. Olsen, M. E. Hildebrandt, R. Urs and A. Furtado; Henri and Flore Lesieur Foundation; Research to Prevent Blindness Department of Ophthalmology; Beauty of Sight Foundation; Florida Lions Eye Bank; Robson Foundation; National Institute of General Medical Sciences (NIH) (T32 GM112601-04).

Acknowledgements

The authors would like to thank Rene Meizoso, and Michael Lupp for assistance in 3D printing the parts necessary for these studies. In addition, we would like to thank Cornelis Rowaan and Alex Gonzalez for help with questions about electronic and design issues, and Dr. Yu-Cherng Channing Chang for advice on data processing and reporting. Finally, the authors would like to thank Dr. Guillermo Amescua for providing feedback on and making possible the clinical aspects of this project.

Jeffrey Peterson was supported in part by NIH Medical Scientist Training Program T32 GM112601-04.

Disclosures

Provisional patent #39756179 filed 6/18/2020, the University of Miami has all rights.

References

1. M. L. Durand, "Bacterial and fungal endophthalmitis," Clin. Microbiol. Rev. **30**(3), 597–613 (2017).
2. A. M. Al-Hatmi, J. F. Meis, and G. S. de Hoog, "Fusarium: Molecular diversity and intrinsic drug resistance," PLoS Pathog **12**(4), e1005464 (2016).
3. J. C. Peterson, H. Durkee, D. Miller, J. Maestre-Mesa, A. Arboleda, M. C. Aguilar, N. Relhan, H. W. J. Flynn, G. Amescua, J.-M. Parel, and E. Alfonso, "Molecular epidemiology and resistance profiles among healthcare- and community-associated staphylococcus aureus keratitis isolates," Infection and drug resistance **12**, 831–843 (2019).
4. A. Arboleda, D. Miller, F. Cabot, M. Taneja, M. C. Aguilar, K. Alawa, G. Amescua, S. H. Yoo, and J.-M. Parel, "Assessment of Rose Bengal versus riboflavin photodynamic therapy for inhibition of fungal keratitis isolates," Am. J. Ophthalmol. **158**(1), 64–70.e2 (2014).
5. F. Halili, A. Arboleda, H. Durkee, M. Taneja, D. Miller, K. A. Alawa, M. C. Aguilar, G. Amescua, H. W. Flynn Jr, and J. M. Parel, "Rose Bengal- and riboflavin-mediated photodynamic therapy to inhibit methicillin-resistant staphylococcus aureus keratitis isolates," Am. J. Ophthalmol. **166**, 194–202 (2016).
6. H. Durkee, A. Arboleda, M. C. Aguilar, J. D. Martinez, K. A. Alawa, N. Relhan, J. Maestre-Mesa, G. Amescua, D. Miller, and J.-M. Parel, "Rose Bengal photodynamic antimicrobial therapy to inhibit pseudomonas aeruginosa keratitis isolates," Lasers Med. Sci. **35**(4), 861–866 (2020).
7. G. Amescua, A. Arboleda, N. Nikpoor, H. Durkee, N. Relhan, M. C. Aguilar, H. W. Flynn, D. Miller, and J.-M. Parel, "Rose Bengal photodynamic antimicrobial therapy: a novel treatment for resistant fusarium keratitis," Cornea **36**(9), 1141–1144 (2017).
8. A. Naranjo, A. Arboleda, J. D. Martinez, H. Durkee, M. C. Aguilar, N. Relhan, N. Nikpoor, A. Galor, S. R. Dubovy, R. Leblanc, H. W. Flynn Jr, D. Miller, J.-M. Parel, and G. Amescua, "Rose Bengal photodynamic antimicrobial therapy for patients with progressive infectious keratitis: a pilot clinical study," Am. J. Ophthalmol. **208**, 387–396 (2019).
9. X. Ragàs, X. He, M. Agut, M. Roxo-Rosa, A. R. Gonsalves, A. C. Serra, and S. Nonell, "Singlet oxygen in antimicrobial photodynamic therapy: photosensitizer-dependent production and decay in E. coli," Molecules **18**(3), 2712–2725 (2013).

Biomedical Optics EXPRESS

10. J. Baier, T. Maisch, M. Maier, M. Landthaler, and W. Baumler, "Direct detection of singlet oxygen generated by UVA irradiation in human cells and skin," J. Invest. Dermatol. **127**(6), 1498–1506 (2007).
11. X. Hua, X. Yuan, A. Di Pietro, and K. R. Wilhelmus, "The molecular pathogenicity of Fusarium keratitis: A fungal transcriptional regulator promotes hyphal penetration of the cornea," Cornea **29**(12), 1440–1444 (2010).
12. P. Huang, T. Tepelus, L. A. Vickers, E. Baghdasaryan, J. Y. Huang, J. A. Irvine, H. Y. Hsu, S. Sadda, and O. L. Lee, "Quantitative analysis of depth, distribution, and density of cysts in Acanthamoeba keratitis using confocal microscopy," Cornea **36**(8), 927–932 (2017).
13. B. Li, H. Lin, D. Chen, B. C. Wilson, and Y. Gu, "Singlet oxygen detection during photosensitization," J. Innov. Opt. Health Sci. **06**(01), 1330002 (2013).
14. J. C. Schlothauer, S. Hackbarth, L. Jäger, K. Drobniewski, H. Patel, S. M. Gorun, and B. Röder, "Time-resolved singlet oxygen luminescence detection under photodynamic therapy relevant conditions: comparison of ex vivo application of two photosensitizer formulations," J. Biomed. Opt. **17**(11), 115005 (2012).
15. P. B. Merkel, R. Nilsson, and D. R. Kearns, "Deuterium effects on singlet oxygen lifetimes in solutions. New test of singlet oxygen reactions," J. Am. Chem. Soc. **94**(3), 1030–1031 (1972).
16. R. L. Jensen, J. Arnbjerg, and P. R. Ogilby, "Reaction of singlet oxygen with tryptophan in proteins: A pronounced effect of the local environment on the reaction rate," J. Am. Chem. Soc. **134**(23), 9820–9826 (2012).
17. J. C. Finlay, S. Mitra, M. S. Patterson, and T. H. Foster, "Photobleaching kinetics of Photofrin in vivo and in multicell tumour spheroids indicate two simultaneous bleaching mechanisms," Phys. Med. Biol. **49**(21), 4837–4860 (2004).
18. J. Moan and K. Berg, "The photodegradation of porphyrins in cells can be used to estimate the lifetime of singlet oxygen," Photochem. Photobiol. **53**(4), 549–553 (1991).
19. M. K. Kuimova, G. Yahioglu, and P. R. Ogilby, "Singlet oxygen in a cell: Spatially dependent lifetimes and quenching rate constants," J. Am. Chem. Soc. **131**(1), 332–340 (2009).
20. P. Wang, F. Qin, Z. G. Zhang, and W. W. Cao, "Quantitative monitoring of the level of singlet oxygen using luminescence spectra of phosphorescent photosensitizer," Opt. Express **23**(18), 22991–23003 (2015).
21. R. W. Redmond and I. E. Kochevar, "Spatially resolved cellular responses to singlet oxygen," Photochem. Photobiol. **82**(5), 1178–1186 (2006).
22. S. Lee, M. E. Isabelle, K. L. Gabally-Kinney, B. W. Pogue, and S. J. Davis, "Dual-channel imaging system for singlet oxygen and photosensitizer for PDT," Biomed. Opt. Express **2**(5), 1233–1242 (2011).
23. N. R. Gemmell, A. McCarthy, B. C. Liu, M. G. Tanner, S. D. Dorenbos, V. Zwiller, M. S. Patterson, G. S. Buller, B. C. Wilson, and R. H. Hadfield, "Singlet oxygen luminescence detection with a fiber-coupled superconducting nanowire single-photon detector," Opt. Express **21**(4), 5005–5013 (2013).
24. B. Hu, N. Zeng, Z. Liu, Y. Ji, W. Xie, Q. Peng, Y. Zhou, Y. He, and H. Ma, "Two-dimensional singlet oxygen imaging with its near-infrared luminescence during photosensitization," J. Biomed. Opt. **16**(1), 016003 (2011).
25. M. J. Niedre, C. S. Yu, M. S. Patterson, and B. C. Wilson, "Singlet oxygen luminescence as an in vivo photodynamic therapy dose metric: validation in normal mouse skin with topical amino-levulinic acid," Br. J. Cancer **92**(2), 298–304 (2005).
26. J. Baier, T. Maisch, M. Maier, M. Landthaler, and W. Baumler, "Direct detection of singlet oxygen generated by UVA irradiation in human cells and skin," J. Invest. Dermatol. **127**(6), 1498–1506 (2007).
27. M. J. Niedre, A. J. Secord, M. S. Patterson, and B. C. Wilson, "In vitro tests of the validity of singlet oxygen luminescence measurements as a dose metric in photodynamic therapy," Cancer Res. **63**, 7986–7994 (2003).
28. B. W. Pogue, J. T. Elliott, S. C. Kanick, S. C. Davis, K. S. Samkoe, E. V. Maytin, S. P. Pereira, and T. Hasan, "Revisiting photodynamic therapy dosimetry: reductionist & surrogate approaches to facilitate clinical success," Phys. Med. Biol. **61**(7), R57–R89 (2016).
29. M. Monici, "Cell and tissue autofluorescence research and diagnostic applications," Biotechnol. Annu. Rev. **11**, 227–256 (2005).
30. S. Lee, D. H. Vu, M. F. Hinds, S. J. Davis, A. Liang, and T. Hasan, "Pulsed diode laser-based singlet oxygen monitor for photodynamic therapy: in vivo studies of tumor-laden rats," J. Biomed. Opt. **13**(6), 064035 (2008).
31. G. Boso, D. Ke, B. Korzh, J. Bouilloux, N. Lange, and H. Zbinden, "Time-resolved singlet-oxygen luminescence detection with an efficient and practical semiconductor single-photon detector," Biomed. Opt. Express **7**(1), 211–224 (2016).
32. I. Mizumoto, "Highly sensitive singlet oxygen spectroscopic system using InGaAs PIN photodiode," in *Developments in Near-Infrared Spectroscopy*, H. Oguma, ed. (IntechOpen, 2017), pp. 65–80.
33. I. Zebger, J. W. Snyder, L. K. Andersen, L. Poulsen, Z. Gao, J. D. C. Lambert, U. Kristiansen, and P. R. Ogilby, "Rapid communication: Direct optical detection of singlet oxygen from a single cell," Photochem. Photobiol. **79**(4), 319–322 (2004).
34. L. K. Andersen, Z. Gao, P. R. Ogilby, L. Poulsen, and I. Zebger, "A singlet oxygen image with 2.5 μm resolution," J. Phys. Chem. A **106**(37), 8488–8490 (2002).
35. O. V. Ovchinnikov, M. S. Smirnov, T. S. Kondratenko, A. S. Perepelitsa, I. G. Grevtseva, and S. V. Aslanov, "Singlet-oxygen sensitization by associates of methylene blue with colloidal Ag2S quantum dots passivated by thioglycolic acid," Opt. Spectrosc. **125**(1), 107–112 (2018).
36. T. J. Moritz, Y. Zhao, M. F. Hinds, J. R. Gunn, J. R. Shell, B. W. Pogue, and S. J. Davis, "Multispectral singlet oxygen and photosensitizer luminescence dosimeter for continuous photodynamic therapy dose assessment during treatment," J. Biomed. Opt. **25**(06), 1–13 (2020).

Biomedical Optics EXPRESS

37. M. M. Kim, R. Penjweini, N. R. Gemmell, I. Veilleux, A. McCarthy, G. Buller, R. H. Hadfield, B. C. Wilson, and T. C. Zhu, "A feasibility study of singlet oxygen explicit dosimetry (SOED) of PDT by intercomparison with a singlet oxygen luminescence dosimetry (SOLD) system," in (2016), Vol. 9694, p. 969406.
38. J. Baier, T. Maisch, J. Regensburger, M. Loibl, R. Vasold, and W. Baeumler, "Time dependence of singlet oxygen luminescence provides an indication of oxygen concentration during oxygen consumption," J. Biomed. Opt. **12**(6), 064008 (2007).
39. C. M. Wertheimer, C. Elhardt, S. M. Kaminsky, L. Pham, Q. Pei, B. Mendes, S. Afshar, and I. E. Kochevar, "Enhancing Rose Bengal-photosensitized protein crosslinking in the cornea," Invest. Ophthalmol. Visual Sci. **60**(6), 1845–1852 (2019).
40. D. Butorina, A. Krasnovsky Jr, and A. Priezzhev, "Study of kinetic parameters of singlet molecular oxygen in aqueous porphyrin solutions. Effect of detergents and the quencher sodium azide," Biofizika **48**, 201–209 (2003).
41. H. T. Atalay, F. Dogruman-Al, F. Sarzhanov, M. C. Özmen, A. B. Tefon, Y. K. Arıbaş, and K. Bilgihan, "Effect of Riboflavin/Rose Bengal-Mediated PACK-CXL on Acanthamoeba Trophozoites and Cysts in Vitro," Curr. Eye Res. **43**(11), 1322–1325 (2018).
42. H. A. Durkee, N. Relhan, A. Arboleda, M. C. Aguilar, K. A. Alawa, F. Halili, C. Rowaan, G. Amescua, H. W. Flynn, D. Miller, and J.-M. A. Parel, "Rose bengal-mediated photodynamic antimicrobial therapy to inhibit *Pseudomonas aeruginosa* isolates in agar plates and contaminated contact lens cases," Invest. Ophthalmol. Visual Sci. **57** (2016).
43. D. Xu and D. C. Neckers, "Aggregation of Rose Bengal molecules in solution," J. Photochem. Photobiol., A **40**(2-3), 361–370 (1987).
44. D. K. Luttrull, O. Valdes-Aguilera, S. M. Linden, J. Paczkowski, and D. C. Neckers, "Rose Bengal aggregation in rationally synthesized dimeric systems," Photochem. Photobiol. **47**(4), 551–557 (1988).
45. M. J. Simpson, H. Poblete, M. Griffith, E. I. Alarcon, and J. C. Scaiano, "Impact of dye-protein interaction and silver nanoparticles on Rose Bengal photophysical behavior and protein photocrosslinking," Photochem. Photobiol. **89**(6), 1433–1441 (2013).
46. O. Valdes-Aguilera and D. C. Neckers, "Aggregation phenomena in xanthene dyes," Acc. Chem. Res. **22**(5), 171–177 (1989).
47. S. M. El-Bashir, I. S. Yahia, M. A. Binhussain, and M. S. AlSalhi, "Designing of PVA/Rose Bengal long-pass optical window applications," Results Phys. **7**, 1238–1244 (2017).
48. D. Borja, F. Manns, P. D. Lamar, A. Rosen, V. Fernandez, and J.-M. Parel, "Preparation and hydration control of corneal tissue strips for experimental use," Cornea **23**(1), 61–66 (2004).
49. D. Borja, F. Manns, P. D. Lamar, A. Rosen, and J.-M. A. Parel, "Effects of immersion solutions on corneal tissue strip hydration and thermal shrinkage," in (2003), Vol. 4951.
50. D. Cherfan, E. E. Verter, S. Melki, T. E. Gisel, F. J. Doyle, G. Scarcelli, S. H. Yun, R. W. Redmond, and I. E. Kochevar, "Collagen cross-linking using Rose Bengal and green light to increase corneal stiffness," Invest. Ophthalmol. Visual Sci. **54**(5), 3426–3433 (2013).
51. A. Naranjo, D. Pelaez, E. Arrieta, E. Salero-Coca, J. D. Martinez, A. L. Sabater, G. Amescua, and J.-M. Parel, "Cellular and molecular assessment of Rose Bengal photodynamic antimicrobial therapy on keratocytes, corneal endothelium and limbal stem cell niche," Exp. Eye Res. **107808** (2019).
52. J. C. Peterson, A. Naranjo, J. D. Martinez, G. Gaidosh, E. Arrieta-Quintero, G. Amescua, and J.-M. Parel, "Rose Bengal depth in human donor cornea after Rose Bengal Photodynamic Antimicrobial Therapy," presented at *American Society for Photobiology 2018 Biennial Meeting*, Tampa, FL, USA (May 12, 2018).
53. E. I. Alarcon, H. Poblete, H. Roh, J.-F. Couture, J. Comer, and I. E. Kochevar, "Rose Bengal binding to collagen and tissue photobonding," ACS Omega **2**(10), 6646–6657 (2017).
54. M. M. Kim, R. Penjweini, N. R. Gemmell, I. Veilleux, A. McCarthy, G. S. Buller, R. H. Hadfield, B. C. Wilson, and T. C. Zhu, "A comparison of singlet oxygen explicit dosimetry (SOED) and singlet oxygen luminescence dosimetry (SOLD) for photofrin-mediated photodynamic therapy," Cancers **8**(12), 109 (2016).
55. M. S. Patterson, S. J. Madsen, and B. C. Wilson, "Experimental tests of the feasibility of singlet oxygen luminescence monitoring in vivo during photodynamic therapy," J. Photochem. Photobiol., B **5**(1), 69–84 (1990).
56. M. Hamaoui, H. Tahi, P. Chapon, B. Duchesne, F. Fantes, W. Feuer, and J. M. Parel, "Corneal preparation of eye bank eyes for experimental surgery," Cornea **20**(3), 317–320 (2001).
57. S. Kling and S. Marcos, "Effect of hydration state and storage media on corneal biomechanical response from in vitro inflation tests," J. Refract. Surg. **29**(7), 490–497 (2013).
58. L. Spadea, G. Maraone, F. Verboschi, E. M. Vingolo, and D. Tognetto, "Effect of corneal light scatter on vision: a review of the literature," Int. J. Ophthalmol. **9**(3), 459–464 (2016).
59. D. A. Peyrot, F. Aptel, C. Crotti, F. Deloison, S. Lemaire, T. Marciano, S. Bancelin, F. Alahyane, L. Kowalczuk, M. Savoldelli, J.-M. Legeais, and K. Plamann, "Effect of incident light wavelength and corneal edema on light scattering and penetration: laboratory study of human corneas," J. Refract. Surg. **26**(10), 786–795 (2010).
60. M. C. Mazzotti, P. Fais, C. Palazzo, F. Fersini, A. Ruggeri, M. Falconi, S. Pelotti, and G. Teti, "Determining the time of death by morphological and immunohistochemical evaluation of collagen fibers in postmortem gingival tissues," Legal Medicine **39**, 1–8 (2019).
61. M. Suarez, T. Martínez Moya, M. Saez, B. Alferez, and M. García-Gallego, "Changes in muscle properties during postmortem storage of farmed sea bream (Sparus aurata)," J. Food Process Eng. **34**(3), 922–946 (2011).

Biomedical Optics EXPRESS

62. M. J. Davies, "Singlet oxygen-mediated damage to proteins and its consequences," Biochem. Biophys. Res. Commun. **305**(3), 761–770 (2003).
63. B. Sjöberg, S. Foley, A. Staicu, A. Pascu, M. Pascu, and M. Enescu, "Protein reactivity with singlet oxygen: Influence of the solvent exposure of the reactive amino acid residues," J. Photochem. Photobiol., B **159**, 106–110 (2016).
64. P. Szpak, "Fish bone chemistry and ultrastructure: implications for taphonomy and stable isotope analysis," J. Archaeological Sci. **38**(12), 3358–3372 (2011).
65. F. Wilkinson, W. P. Helman, and A. B. Ross, "Rate constants for the decay and reactions of the lowest electronically excited singlet state of molecular oxygen in solution. An expanded and revised compilation," J. Phys. Chem. Ref. Data **24**(2), 663–677 (1995).
66. R. F. Brubaker, W. M. Bourne, L. A. Bachman, and J. W. McLaren, "Ascorbic acid content of human corneal epithelium," Invest. Ophthalmol. Visual Sci. **41**, 1681–1683 (2000).
67. G. G. Kramarenko, S. G. Hummel, S. M. Martin, and G. R. Buettner, "Ascorbate reacts with singlet oxygen to produce hydrogen peroxide," Photochem. Photobiol. **82**(6), 1634–1637 (2006).
68. D. K. Sardar, B. G. Yust, F. J. Barrera, L. C. Mimun, and A. T. C. Tsin, "Optical absorption and scattering of bovine cornea, lens and retina in the visible region," Lasers Med. Sci. **24**(6), 839–847 (2009).
69. P. G. Seybold, M. Gouterman, and J. Callis, "Calorimetric, photometric and lifetime determinations of fluorescence yields of fluorescein dyes*," Photochem. Photobiol. **9**(3), 229–242 (1969).
70. B. G. Yust, L. C. Mimun, and D. K. Sardar, "Optical absorption and scattering of bovine cornea, lens, and retina in the near-infrared region," Lasers Med. Sci. **27**(2), 413–422 (2012).
71. B. Nemati, H. G. Rylander, and A. J. Welch, "Optical properties of conjunctiva, sclera, and the ciliary body and their consequences for transscleral cyclophotocoagulation," Appl. Opt. **35**(19), 3321–3327 (1996).
72. B. Nemati, H. G. Rylander, and A. Welch, "Optical properties of conjunctiva, sclera, and the ciliary body and their consequences for transscleral cyclophotocoagulation: erratum," Appl. Opt. **36**(1), 416 (1997).
73. J. C. Schlothauer, J. Falckenhayn, T. Perna, S. Hackbarth, and B. Röder, "Luminescence investigation of photosensitizer distribution in skin: correlation of singlet oxygen kinetics with the microarchitecture of the epidermis," J. Biomed. Opt. **18**(11), 115001 (2013).
74. T. D. Poulsen, P. R. Ogilby, and K. V. Mikkelsen, "Solvent effects on the O2(a1Δg)−O2(X3Σg-) radiative transition: comments regarding charge-transfer interactions," J. Phys. Chem. A **102**(48), 9829–9832 (1998).
75. P. R. Ogilby and C. S. Foote, "Chemistry of singlet oxygen. 42. Effect of solvent, solvent isotopic substitution, and temperature on the lifetime of singlet molecular oxygen (1.DELTA.g)," J. Am. Chem. Soc. **105**(11), 3423–3430 (1983).